High performance poly-Si TFTs fabricated by continuous-wave laser annealing of metal-induced lateral crystallised silicon films

C.-P. Chang and Y.S. Wu

In this process, amorphous silicon was first transformed to polycrystalline silicon (poly-Si) using a metal-induced lateral crystallisation (MILC) process, followed by annealing with a continuous-wave laser lateral ($\lambda \sim 532$ nm) crystallisation (CLC) with an output power of 3.8 W. MILC-CLC-TFT performed far superior to MILC-TFT. The mobility of the MILC-CLC-TFT was 293 $\mathrm{cm^2/Vs}$, which was much higher than that of MILC TFTs (54.8 $\mathrm{cm^2/Vs}$). In addition, MILC-CLC TFTs showed better device uniformity and reliability.

Introduction: Low-temperature polycrystalline silicon (LTPS) is very important for device applications such as solar cells and thin-film transistors (TFTs) [1]. Therefore, intensive studies have been carried out to reduce the crystallisation temperature of amorphous silicon (α-Si).

Among many methods, metal-induced lateral crystallisation (MILC) and excimer laser crystallisation (ELC) appear to be very promising methods [2–4]. MILC has the merits of low cost and uniform crystallisation over a large area. However, not all α-Si film was transformed to crystal Si [2, 3]. The ELC technique appears to be highly promising unfortunately their uniformity is inadequate and the surfaces of their poly-Si films are rough [4]. To improve the uniformity and performance of ELC-TFTs, many methods have been proposed [5–7]. The cost of the ELC system, however, is still high.

Recently, continuous-wave (CW) laser lateral crystallisation (CLC) of amorphous Si has been developed for LTPS TFT [8, 9]. Not only are the performances of CLC TFT better, but the manufacturing cost is lower than ELC TFTs. In this Letter, a new manufacturing method using post-annealing of MILC poly-Si TFTs with a CW laser (MILC-CLC) is proposed.

Experiment: The MILC process began with 4-inch quartz wafer substrates where wet oxide films of 500 nm were grown. A silane-based undoped amorphous silicon (α-Si) layer with a thickness of 100 nm was deposited using low-pressure chemical vapour deposition (LPCVD). The photoresist was patterned to form the desired Ni lines, and a 20 Å-thick Ni film was deposited on the α-Si. The samples were then dipped into acetone for 5 min to remove the photoresist. Samples were subsequently annealed at 540°C for 18 h to form the MILC poly-Si film. The unreacted Ni metal was removed by chemical etching. The MILC poly-Si films were then irradiated by a CW laser ($\lambda \sim 532$ nm) with various output powers (2.5, 3.8, 5 W) in an air atmosphere to fabricate the MILC-CLC poly-Si. Reactive ion etching (RIE) was employed to form islands of poly-Si regions. Next, a 100 nm-thick oxide layer was deposited as the gate insulator by plasma-enhanced chemical vapour deposition (PECVD). A 200 nm-thick poly-Si film was then deposited for gate electrodes by LPCVD. After defining the gate, self-aligned phosphorous ions were implanted to form the source/drain and gate. The dopant activation was performed at 600°C in N_2 ambient for 24 h.

Results and discussions: Fig. 1*a* shows an SEM image of the Secco-etched MILC needle grains. Most of the grains were parallel to each other in the <111> direction [10]. The width of the needlelike grains was around 50 nm. Among these grains remained some uncrystallised α-Si regions, which had been etched away. To fabricate MILC-CLC poly-Si films, MILC films were irradiated using a CW laser with the scan direction parallel to the needlelike poly-Si grains. When the laser output power was 2.5 W, the sizes and shapes of the needle Si grains were similar to those of MILC poly-Si (Fig. 1*a*). This is because MILC-CLC films were in the amorphous-melting regime. Only the α-Si regions among Si grains were melted. When the output power reached 3.8 W, the width of the grains increased markedly from 50 nm to ~3 μm, as shown in Fig. 1*b*. The large grains were only molten partially and served as the nuclei for growth. The width of these grains markedly increased to ~3 μm owing to the geometrical coalescence of Si needle grains [11]. The grain boundary between grains disappears, resulting in the sudden development of a much larger grain. This coalescence is an important phenomenon for grains having a strong preferred orientation (MILC needle grains had a strong preferred orientation <111>). In this study, the effect of the CW ($\lambda = 532$ nm) laser post-annealing was much better than that of the excimer laser. The width of the Si grains dramatically increased to ~3 μm (the grains ranged from 2.5 to 4 μm), while that of excimer laser post-annealing was only 600 nm [10]. When the laser power was 5 W, the width of the grains ranged from 3 to 12 μm. The uniformity of the grain size was poor. As a result, device performances were not uniform. To achieve high performance with good uniformity, the CW laser with an output power of 3.8 W was chosen to fabricate MILC-CLC TFTs.

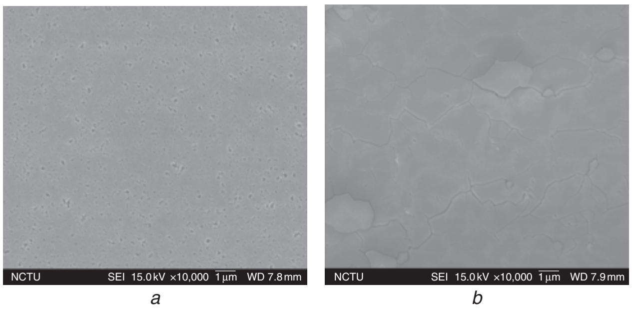

Fig. 1 *SEM images of MILC and MILC-CLC poly-Si grains*

a MILC
b MILC-CLC

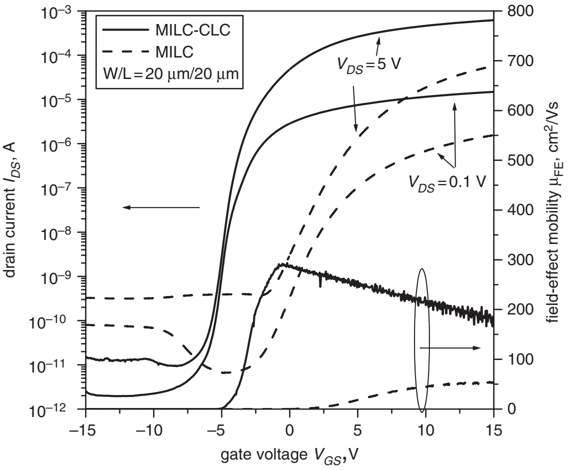

Fig. 2 *Typical I_{DS}-V_{GS} transfer characteristics and field-effect motilities of MILC and MILC-CLC TFTs*

Fig. 2 shows the transfer characteristics and field-effect mobility against the gate voltage of MILC-CLC and MILC TFTs. The measured and extracted key device parameters are summarised in Table 1. MILC-CLC TFTs exhibited field-effect mobility reaching 293 $\mathrm{cm^2/Vs}$, which was much higher than that of MILC TFTs. The subthreshold slope (SS) and V_{TH} of the MILC-CLC TFTs were 0.39 V/dec. and −4.54 V, which were superior to 1.42 V/dec. and 2.24 V of the MILC TFTs. The ON/OFF current ratios of the MILC-CLC and MILC poly-Si TFTs were 6.69×10^7 and 0.18×10^6 at $V_{DS} = 5$ V, respectively.

Table 1: Device characteristics of MILC and MILC-CLC TFTs

Device parameters	MILC-CLC	MILC
Field-effect mobility ($\mathrm{cm^2/Vs}$)	293	54.8
Subthreshold slope (V/dec.)	0.39	1.42
Threshold voltage V_{TH} (V)	−4.54	2.24
ON/OFF current ratio	6.69×10^7	0.18×10^6

As mentioned earlier, many intragrain defects and α-Si regions remained among MILC poly-Si grains. These defects trap charge carriers and degrade electric performance. MILC-CLC TFTs do not have these problems because, as presented in Fig. 1*b*, the width Si of MILC-CLC grains dramatically increased to 3 μm. Most of these geometrical coalescence grains and their boundaries are parallel to the drain current (I_{ds}), reducing the impedance to carrier flow and thereby reducing the threshold voltage and greatly increasing the mobility and I_{on}/I_{off} current ratio.

Twenty MILC-CLC TFTs were measured in μ_{FE} and V_{TH} to investigate device uniformity. The standard deviations of the μ_{FE} and V_{TH} are 7.46 and 0.165, respectively. As a result, small standard deviations of MILC-CLC TFTs indicate a fine uniformity owing to the CW laser annealing. The other important issue of MILC-CLC poly-Si TFTs is their reliability, which was examined under hot-carrier stress (HCS). Fig. 3 shows the field-effect mobility and threshold voltage variation against stress time, and the stress condition is $V_{D,stress} = 15$ V, $V_{G,stress} = V_{GS} - V_{TH} = 15$ V for varied time duration. It is found that MILC-CLC TFTs also had a good reliability.

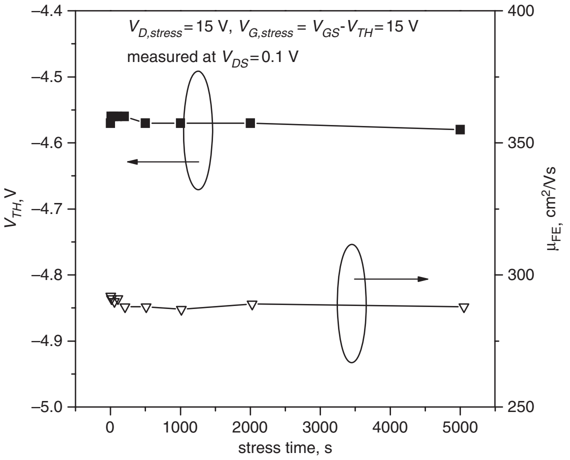

Fig. 3 *Field-effect mobility and threshold voltage variation examined under hot-carrier stress*

Conclusions: A high-performance LTPS TFT fabricated by MILC-CLC was investigated. In this process, amorphous silicon was first transformed to poly-Si using an MILC method, and then annealed using a continuous-wave laser. Laser-annealing with an output power of 3.8 W greatly increased the width of the needle grains from 50 nm to 3 μm by geometrical coalescence. MILC-CLC-TFT markedly outperformed that of the MILC-TFT because the MILC-CLC poly-Si film had much larger grains and fewer intragrain defects than the MILC poly-Si film. The MILC-CLC-TFT has a lower threshold voltage, smaller subthreshold slope and a higher on/off current ratio than the MILC-TFT. The mobility of the MILC-CLC-TFT was 293 cm^2/Vs, which was much higher than that of MILC TFTs (54.8 cm^2/Vs). Besides, MILC-CLC TFTs showed better device uniformity and reliability.

Acknowledgments: This project was funded by the Sino American Silicon Products Incorporation and the National Science Council of the Republic of China under grant no. 95-2221-E009-087-MY3. Technical supports from the National Nano Device Laboratory, Center for Nano Science and Technology and the Nano Facility Center of the National Chiao Tung University are acknowledged.

7 June 2008
Electronics Letters online no: 20081620
doi: 10.1049/el:20081620

C.-P. Chang and Y.S. Wu (*Department of Material Science and Engineering, National Chiao Tung University, 1001 Ta-Hsueh Road, Hsinchu, Taiwan, Republic of China*)

E-mail: sermonwu@stanfordalumni.org

References

1 Stewart, M., Howell, R.S., Pires, L., and Hatalis, M.K.: 'Polysilicon TFT technology for active matrix OLED displays', *IEEE Trans. Electron Devices*, 2001, **48**, (5), pp. 845–851
2 Lee, S.W., and Joo, S.K.: 'Low temperature poly-Si thin-film transistor fabrication by metal-induced lateral crystallization', *IEEE Electron Device Lett.*, 1996, **17**, (4), pp. 160–162
3 Meng, Z., Wang, M., and Wong, M.: 'High performance low temperature metal-induced unilaterally crystallized polycrystalline silicon thin film transistors for system-on-panel applications', *IEEE Trans. Electron Devices*, 2000, **47**, (2), pp. 404–409
4 Giust, G.K., Sigmon, T.W., Boyce, J.B., and Ho, J.: 'High-performance laser-processed polysilicon thin-film transistors', *IEEE Electron Device Lett.*, 1999, **20**, (2), pp. 77–79
5 Jeon, J.H., Lee, M.C., Park, K.C., and Han, M.K.: 'A new polycrystalline silicon TFT with a single grain boundary in the channel', *IEEE Electron Device Lett.*, 2001, **22**, (9), pp. 429–431
6 Kim, C.H., Song, I.H., Nam, W.J., and Han, M.K.: 'A poly-Si TFT fabricated by excimer laser recrystallization on floating active structure', *IEEE Electron Device Lett.*, 2002, **23**, (6), pp. 315–317
7 Chen, T.F., Yeh, C.F., Liu, C.Y., and Lou, J.C.: 'A novel four-mask-processed poly-Si TFT fabricated using excimer laser crystallization of an edge-thickened α-Si active island', *IEEE Electron Device Lett.*, 2004, **25**, (6), pp. 396–398
8 Lin, Y.T., Chen, C., Shieh, J.M., Lee, Y.J., and Pan, C.L.: 'Stability of continuous-wave laser-crystallized eplike silicon transistors', *Appl. Phys. Lett.*, 2007, **90**, (7), p. 073508
9 Hara, A., Takei, M., Takeuchi, F., Suga, K., Yoshino, K., Chida, M., Kakehi, T., Ebiko, Y., Sano, Y., and Sasaki, N.: 'High performance low temperature polycrystalline silicon thin film transistors on non-alkaline glass produced using diode pumped solid state continuous wave laser lateral crystallization', *Jpn. J. Appl. Phys.*, 2004, **43**, (4A), pp. 1269–1276
10 Hu, G.R., Wu, Y.S., Chao, C.W., and Shih, H.C.: 'Growth mechanism of laser annealing of nickel-induced lateral crystallized silicon films', *Jpn. J. Appl. Phys.*, 2006, **45**, (1A), pp. 21–27
11 Robert, E., Hill, R., and in Abbaschian, R.: 'Physical metallurgy principles' (Thomoson, Boston, MA, 1992, 3rd edn.), Chap. 8, p. 254